Plasmon-Enhanced Photocatalytic CO_2 Conversion within Metal-Organic Frameworks Under Visible Light

Kyung Min Choi,[†,§,⊥,#] Dohyung Kim,[‡,‖,#] Bunyarat Rungtaweevoranit,[†,§] Christopher A. Trickett,[†,§] Jesika Trese Deniz Barmanbek,[†] Ahmad S. Alshammari,[¶] Peidong Yang,*[,†,‡,□,‖] and Omar M. Yaghi*[,†,§,‖,¶]

[†]Department of Chemistry, [‡]Department of Materials Science and Engineering, and [‖]Kavli Energy NanoSciences Institute, University of California, Berkeley, California 94720, United States

[§]Materials Sciences Division, and [□]Chemical Sciences Division, Lawrence Berkeley National Laboratory, Berkeley, California 94720, United States

[⊥]Department of Chemical and Biological Engineering, Sookmyung Women's University, Seoul 04310, Korea

[¶]King Abdulaziz City for Science and Technology, Riyadh 12371, Saudi Arabia

*Corresponding authors. E-mail: p_yang@berkeley.edu (P.Y); yaghi@berkeley.edu (O.M.Y)

[#]These authors contributed equally to this work

Table of Contents

Supporting Section S1 *Materials and methods*

Materials

Chemicals used in this work. All reagents, unless otherwise stated, were obtained from commercial sources (Sigma-Aldrich) and were used without further purification. Specifically, H_2BPDC (BPDC = 4,4′-biphenyldicarboxylate), H_2BPYDC (BPYDC = 2,2'-bipyridine-5,5'–dicarboxylate), pentacarbonylchlororhenium(I), anhydrous acetonitrile, triethylamine, 1,5-pentanediol, copper(II) chloride, silver nitrate and PVP (M_w ~55,000 and M_w ~40,000) were purchased from Aldrich. $Cu(acac)_2$ was purchased from Strem Chemicals. *N,N*-Dimethylformamide (DMF), formic acid, acetic acid and methanol was obtained from EMD Millipore Chemicals. *N,N*-diethylformamide (DEF, BASF) solvent was purified by filtration through a column filled with activated carbon (Calgon) and silica gel (EMD, silica gel 60).

Methods

Single crystals of $Zr_6O_4(OH)_4(Re(CO)_3Cl\text{-}BPYDC)_{0.72}(BPDC)_{5.28}$, Re_3-MOF: H_2ReTC (1.800 mg, 0.003 mmol), H_2BPDC (2.907 mg, 0.012 mmol), and $ZrOCl_2\cdot8H_2O$ (3.040 mg, 0.009 mmol) were dissolved in a solvent mixture of DEF/formic acid (0.2 mL/3.3 mL) in a 20 mL vial. The mixture was heated at 140 °C for 12 h. Red octahedral crystals were collected and washed three times with 5 mL of fresh DMF. Single-crystal X-ray diffraction (SXRD) data for Re_3-MOF are detailed in Supporting Information.

Synthesis of Cu nanoparticle. In a 50 mL 3-neck round bottom flask, a solution of 654 mg of $Cu(acac)_2$ and 500 mg of polyvinylpyrrolidone (MW 40,000) in 25 mL of 1,5-pentanediol was heated at 120 °C under vacuum for 25 min using a heating mantle equipped with a temperature controller. The flask was refilled with nitrogen and the temperature was increased rapidly to 220 ºC which was then kept constant for 30 min. The synthesized Cu NPs were cooled down and washed twice with ethanol and once with DMF using a centrifuge (9000 rpm, 10 min). The Cu NPs were then redispersed in DMF (3 mg/mL).

Synthesis of Cu$\subset$Re$_2$-MOF. A Re-MOF stock solution was prepared by dissolving H_2BPDC (9.110 mg, 0.037 mmol), H_2ReTC (1.320 mg, 0.002 mmol), 70 wt. % Zr(OPr)$_4$ in 1-propanol (18 µl, 0.04 mmol), and acetic acid (0.5 ml, 8.7 mmol) in 10 ml DMF. 2 mL of the Cu nanoparticle solution was added to the frozen solution of 1.25 ml of the Re-MOF stock solution, 8.75 ml of DMF, and 0.050 ml of acetic acid in a 25 ml Schlenk flask. The solution was degassed by freeze-pump-thaw for 3 cycles. Then the reaction was heated to 90 °C in a preheated oil bath for 25 min. The orange-red solid was collected by centrifugation (8000 rpm, 5 min), redispersed in acetonitrile and frozen dried using a lyophilizer. The dried product was washed three times with DMF using a centrifuge (8000 rpm for 5 min) and sonication, and then sequentially immersed in anhydrous acetonitrile for three 24 h periods.

Synthesis of Ag$\subset$Re$_0$-MOF: Ag nanocube particles were washed three times with DMF using a centrifuge (9000 rpm for 10 min) and concentrated to a 3 mg/ml Ag nanocube solution. A Re-MOF stock solution was prepared by dissolving H_2BPDC (9.768 mg, 0.040 mmol), $ZrCl_4$ (9.320 mg, 0.040 mmol), and acetic acid (0.500 ml, 8.700 mmol) in 10 ml DMF. Then 2.1 ml of the Re-MOF stock solution and 2 ml of the Ag nanocube solution were combined with 1 ml DMF containing 0.125 ml acetic acid in a 20 ml vial with a magnetic stirrer and heated at 90 °C in an aluminum heating block with vigorous stirring for 30 min. The precipitate was collected and washed three times with DMF using a centrifuge (9000 rpm for 10 min) and sonication, then sequentially immersed in anhydrous acetonitrile for three 24 h periods.

Supporting Section S2 *Structural analysis of single-crystalline* Re_3*-MOF*

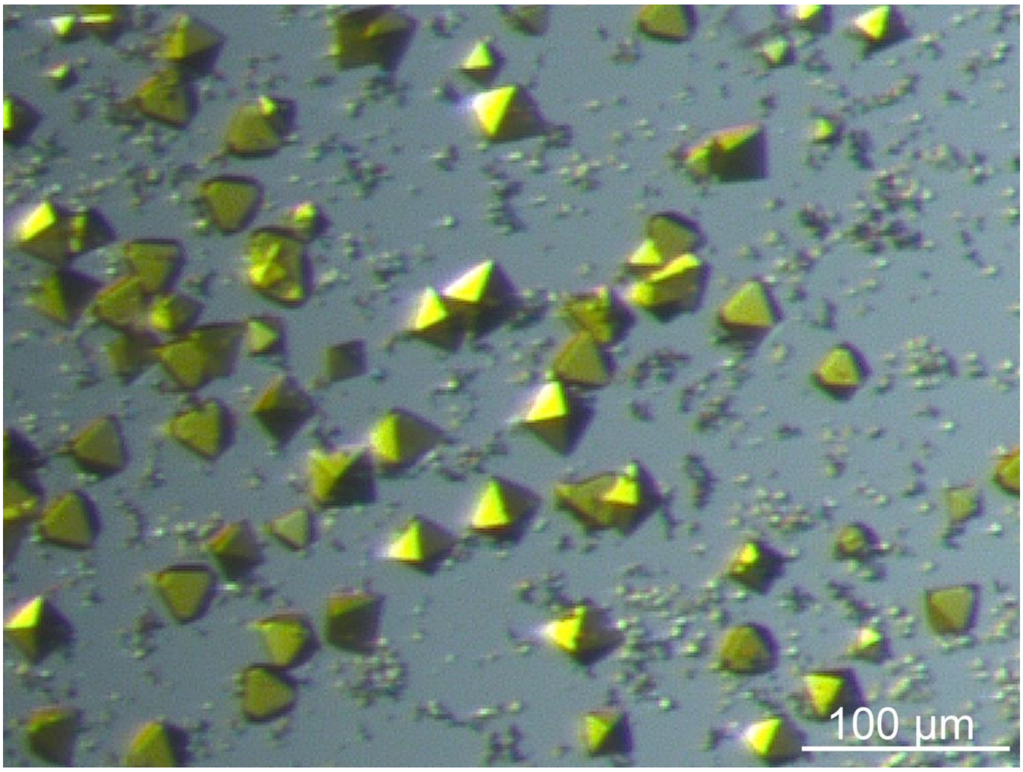

Supporting Figure S1. Optical image of single crystalline Re_3-MOF

Single-crystal X-ray diffraction (SXRD) data for the structure containing 3 complexes of Re per unit cell was collected on beamline 11.3.1 at the Advanced Light Source, Lawrence Berkeley National Lab. The sample was mounted on a MiTeGen® kapton loop and placed in a 100(2) K nitrogen cold stream provided by an Oxford Cryostream 700 Plus low temperature apparatus on the goniometer head of a Bruker D8 diffractometer equipped with a PHOTON100 CMOS detector operating in shutterless mode. Diffraction data were collected using synchrotron radiation monochromated using silicon (111) to a wavelength of 0.7749(1) Å. An approximate full-sphere of data was collected using a combination of phi and omega scans with scan speeds of 1 second per degree for the phi scans, and 1 and 2 seconds per degree for the omega scans at $2\theta = 0$ and -45, respectively. The structure was solved by intrinsic phasing (SHELXT) and refined by full-matrix least squares on F^2 (SHELXL-2014).

Table S1 | Crystal structure data for Re_3-MOF

Compound	**Re_3-MOF**
chemical formula	$C_{92.88}H_{28}Cl_{0.72}N_{5.52}O_{36}Re_{0.78}Zr_6$
formula mass	2515.13
crystal system	cubic
space group	*Fm-3m*
λ (A)	0.7749(1)
a (A)	26.7213(8)
Z	4
V (A^3)	19079.8(17)
temperature (K)	100(2)
size /mm	0.020 x 0.020 x 0.020
density (g/cm^{-3})	0.876
measured reflections	51150
unique reflections	782
parameters	70
restraints	4
R_{int}	0.1671
θ range (deg)	2.35-25.91
R_1, wR_2	0.0631, 0.2292
S (GOF)	1.185
max/min res. dens. (e/A^3)	1.38/-0.65

All non-hydrogen atoms were refined anisotropically unless otherwise specified. Hydrogen atoms were geometrically calculated and refined as riding atoms. Efforts were made to avoid the use of solvent masking despite the porous nature of the structure. Disordered *N,N*-diethylformamide was modeled as hydrogen bonding to the μ^3-OH group on the zirconium oxide cluster. The remaining solvent molecules are too disordered to be modeled, though a residual electron density peak of 1.4 e $Å^{-3}$ is observed in the cavity of the framework. This was not modeled as it is part of the highly disordered solvent molecules, and cannot be assigned with meaningful information.

The chloride bonded to rhenium, despite its low occupancy, is observed in the difference map in the axial position. Additional evidence supporting the presence and position of chloride are obtained from the UV-vis, IR spectra and digested ^{1}H NMR (see Supporting Figs. 3-5).

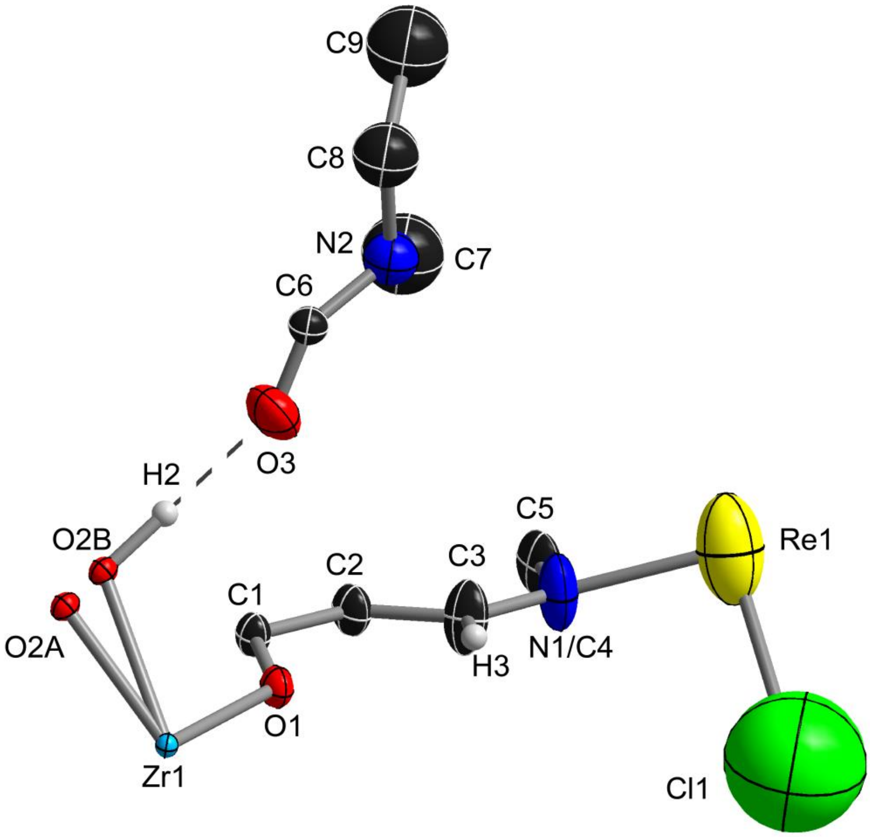

Supporting Figure S2. Asymmetric unit of the single crystal Re$_3$-MOF, with *N*,*N*-diethylformamide hydrogen bonding to the zirconium oxide cluster. Due to low occupancy, only Cl (Chloride) and not CO could be located on ReTC. Hydrogen atoms were not placed on DEF due to low occupancy and heavy disorder. Labeling is as follows: zirconium in cyan, oxygen in red, carbon in black, hydrogen in white, nitrogen in royal blue, rhenium in yellow, chlorine in green.

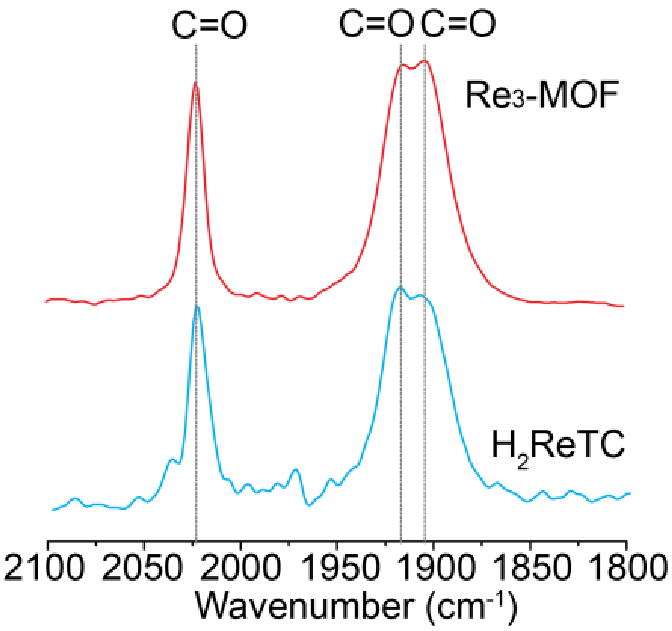

Supporting Figure S3. Infrared (IR) spectra of Re_3-MOF and H_2ReTC

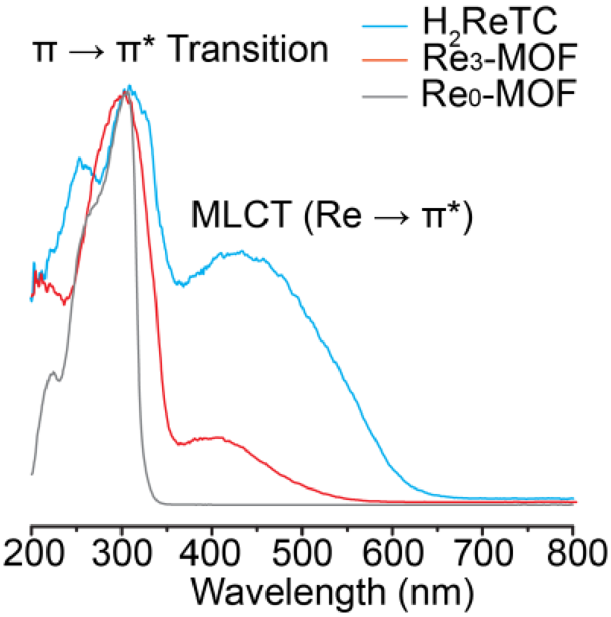

Supporting Figure S4. Ultraviolet-visible (UV-Vis) spectra of Re_3-MOF, Re_0-MOF and H_2ReTC

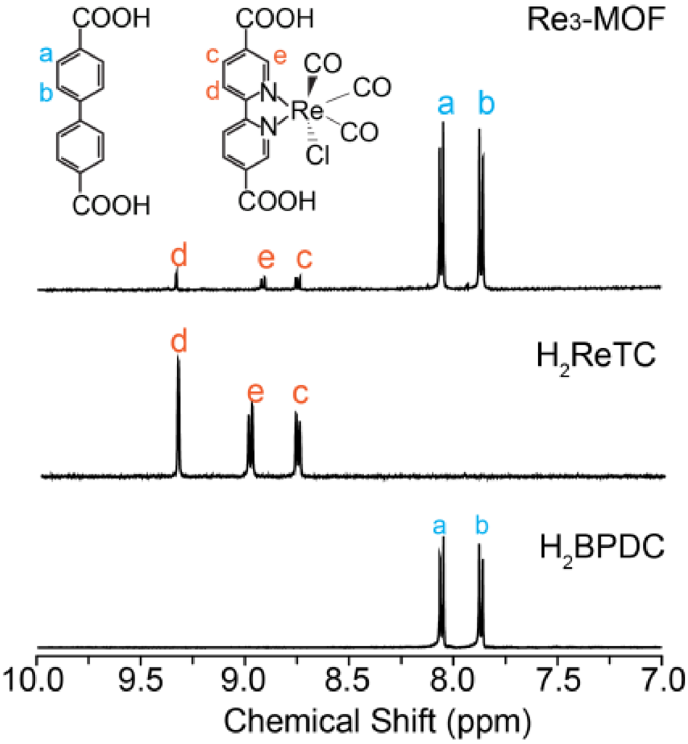

Supporting Figure S5. ^{1}H NMR spectra of Re$_3$-MOF (top), H$_2$ReTC (middle), and H$_2$BPDC (bottom)

Supporting Section S3. *Characterization of Re$_n$-MOFs*

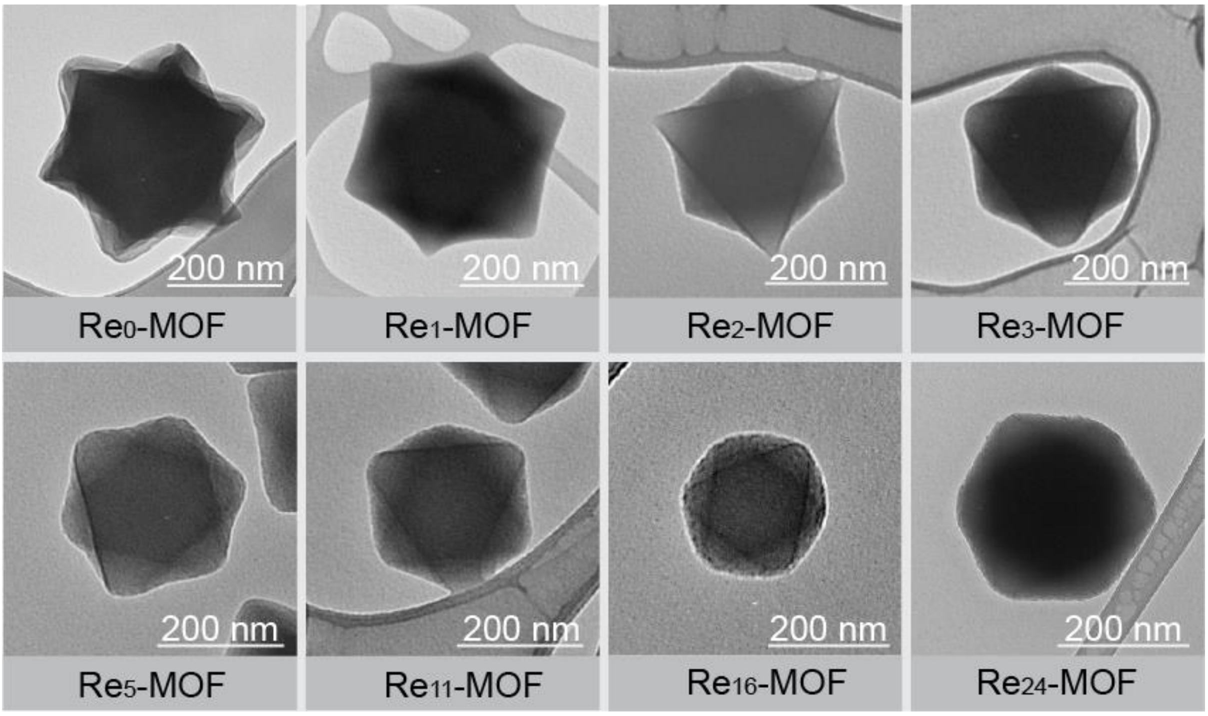

Supporting Figure S6. TEM images of Re$_n$-MOFs

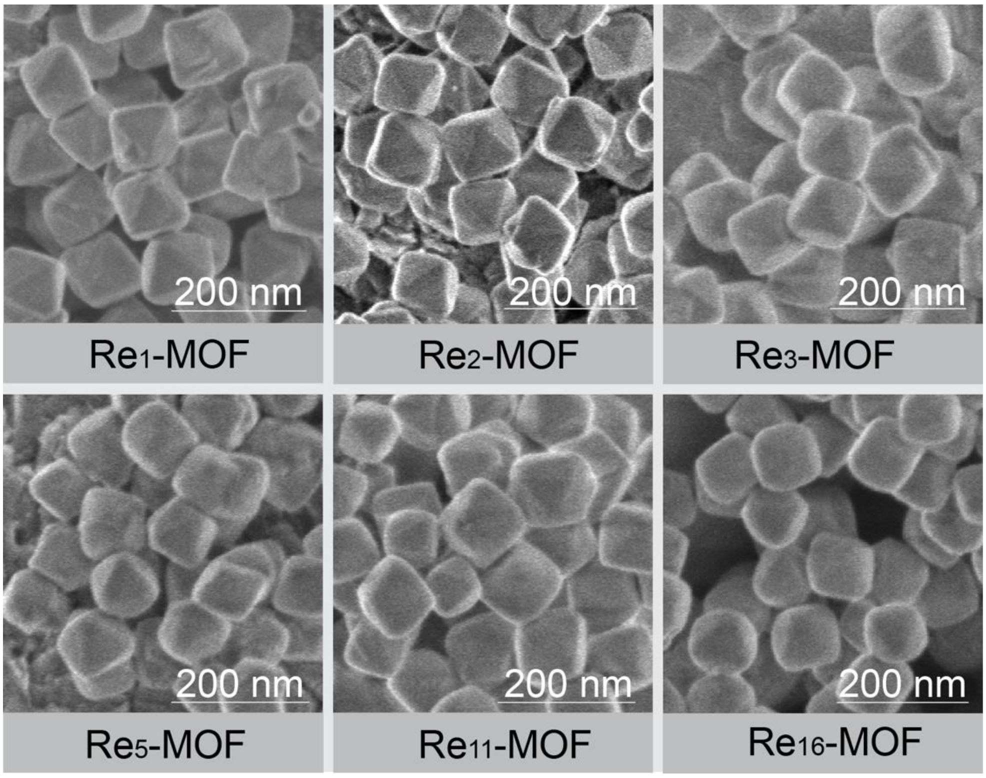

Supporting Figure S7. SEM images for Re$_n$-MOFs

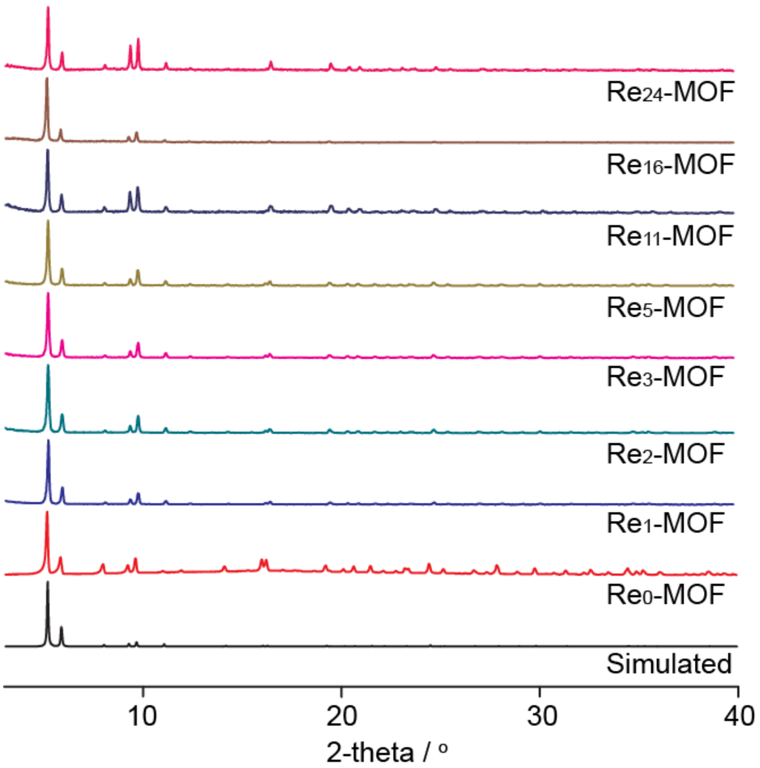

Supporting Figure S8. PXRD of Re$_n$-MOFs

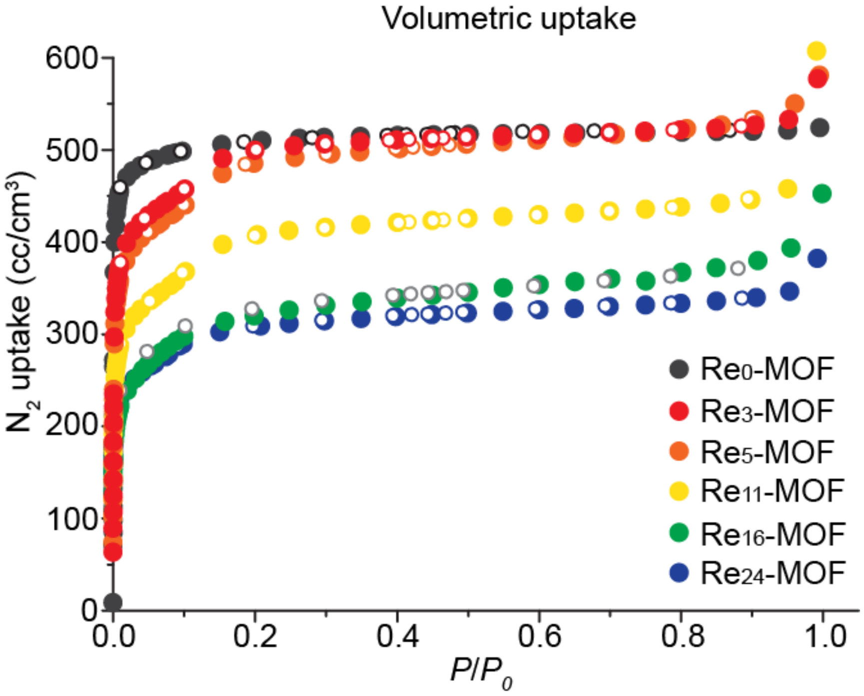

Supporting Figure S9. N_2 sorption isotherms for Re$_n$-MOFs at 77 K with adsorption and desorption points represented by closed and open circles, respectively (P/P_0, relative pressure).

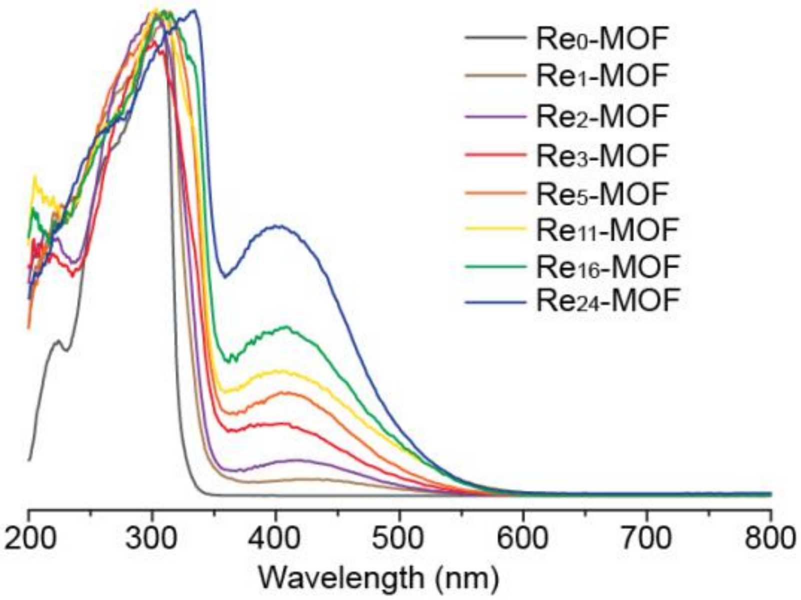

Supporting Figure S10. UV-Vis spectra of Re_n-MOFs. Rise in the absorption intensity in the visible region is due to larger fraction of ReTC linkers in Re_n-MOFs. Both BPDC and ReTC have characteristic absorption in the UV region from biphenyl and bipyridine units. However, ReTC features visible absorption from MLCT, so that rising density of ReTC in Re_n-MOFs results in the increased absorption in the visible range relative to the UV region.

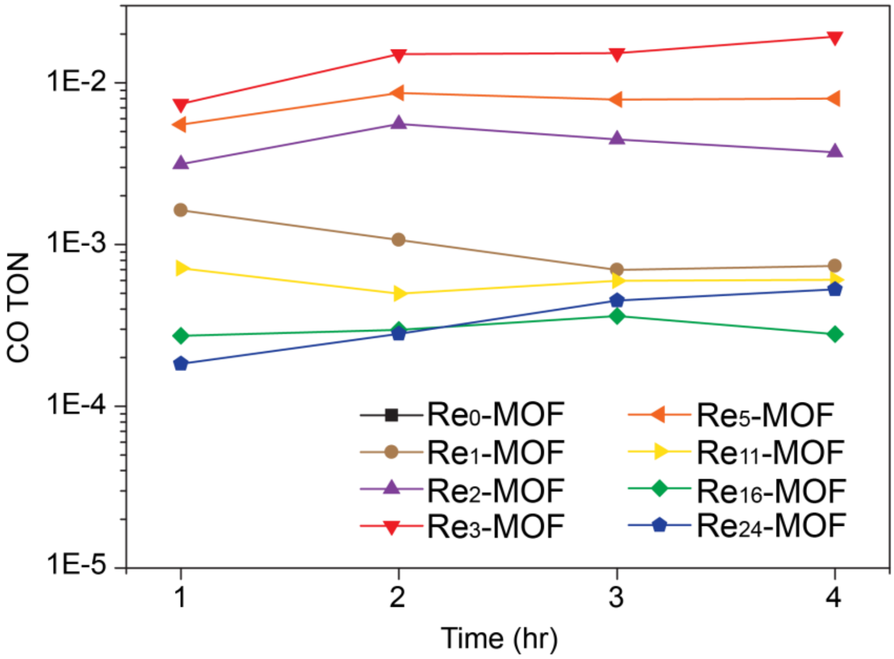

Supporting Figure S11. Photocatalytic CO_2-to-CO conversion activity of Re_n-MOFs (Note : the only product observed was CO)

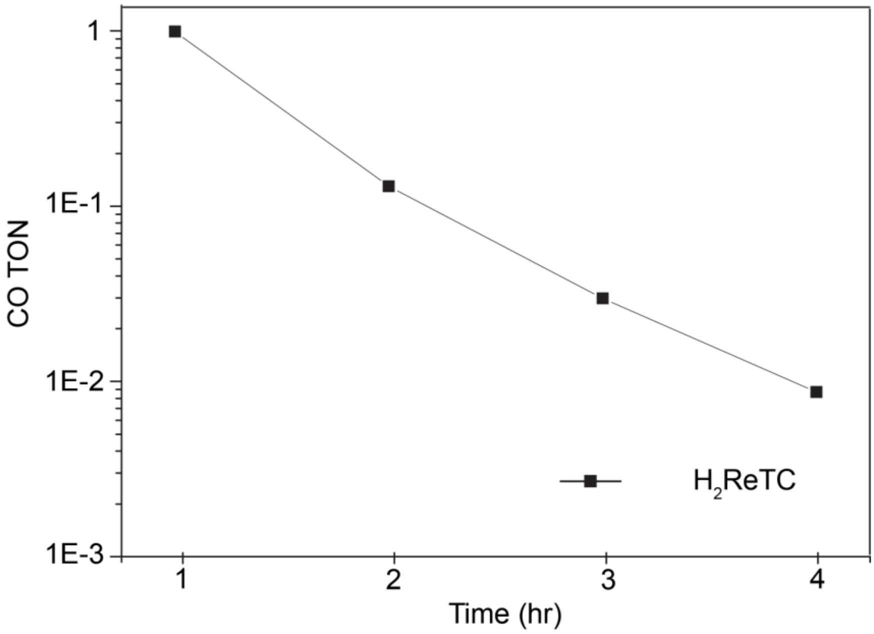

Supporting Figure S12. Photocatalytic CO_2-to-CO conversion activity of H_2ReTC (96% selectivity to CO observed)

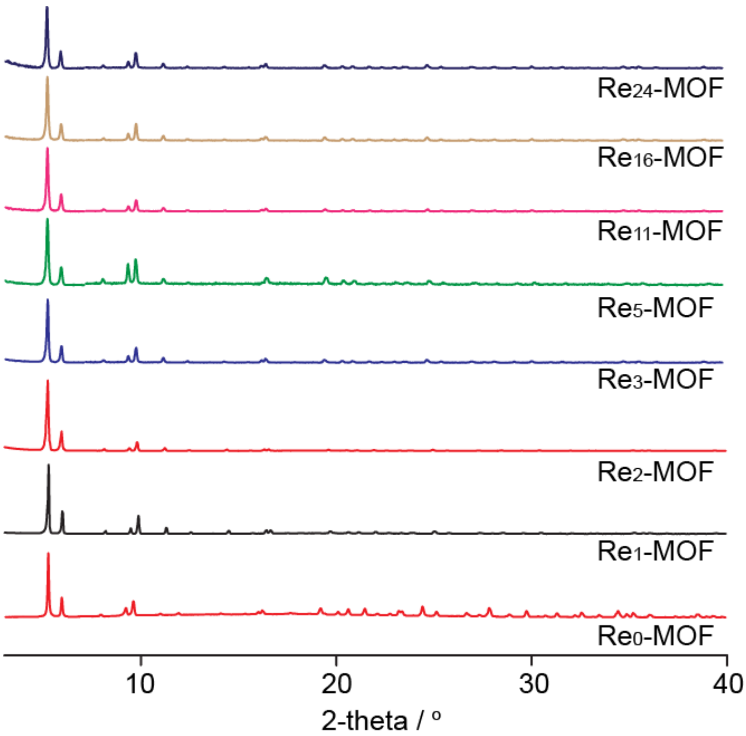

Supporting Figure S13. PXRD of Re$_n$-MOFs after photocatalysis

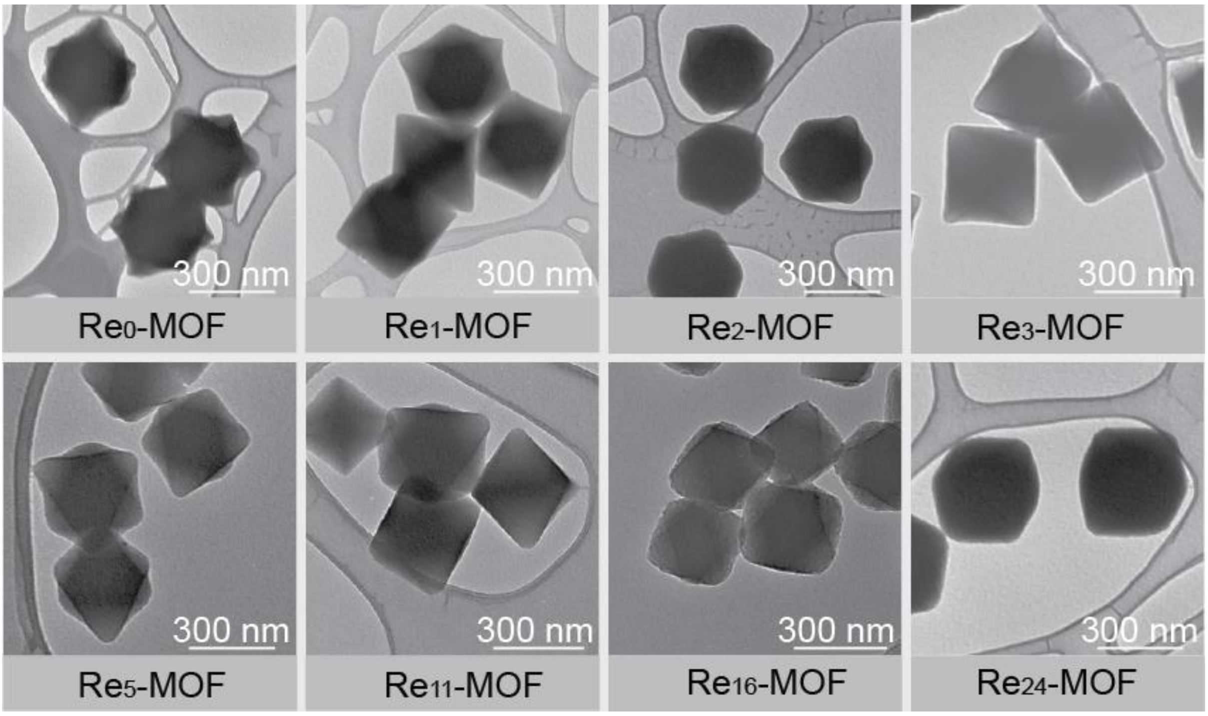

Supporting Figure S14. TEM images of Re$_n$-MOFs after photocatalysis

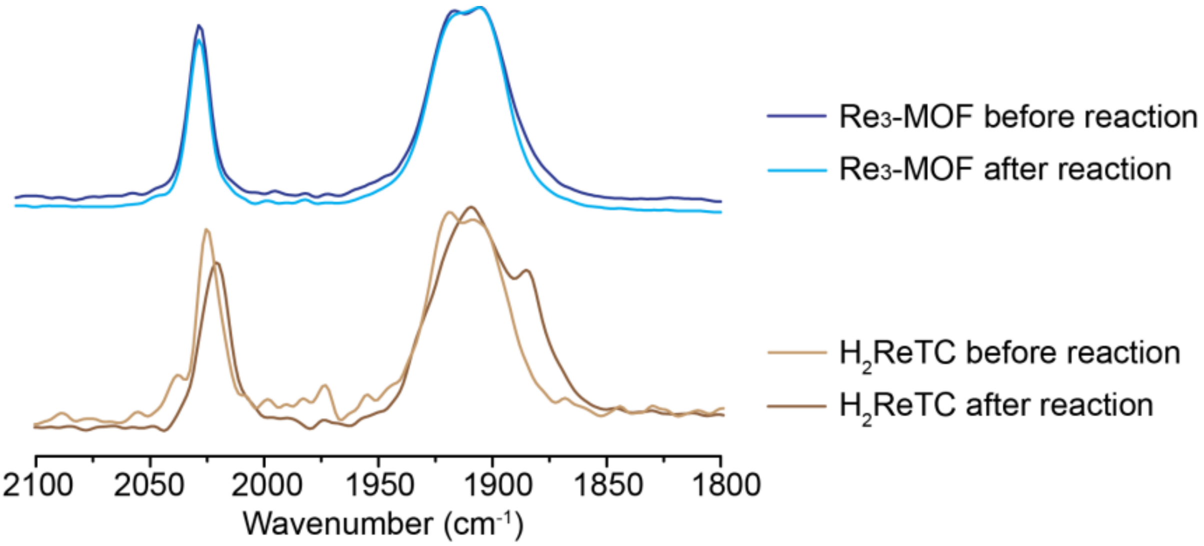

Supporting Figure S15. IR spectra of Re_3-MOF and H_2ReTC before and after photocatalysis

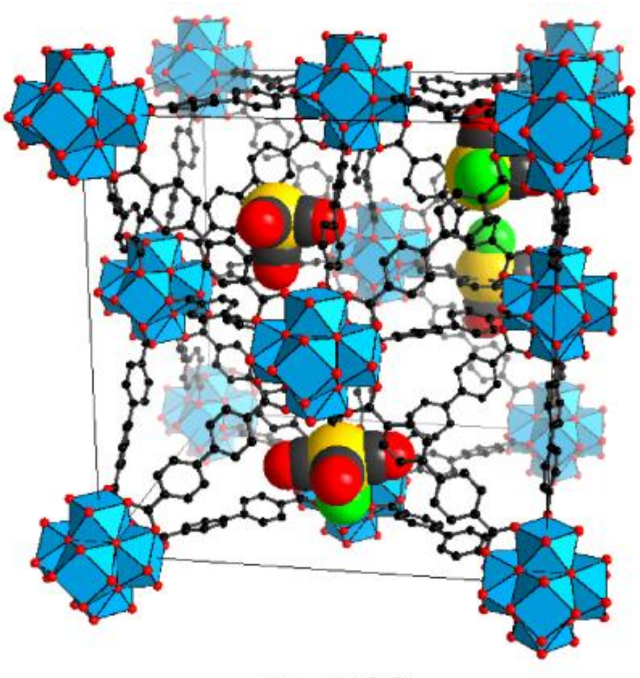

Supporting Figure S16. Structural model of Re_4-MOF with each octahedral pore being occupied with a single ReTC complex (4 ReTCs per unit cell).

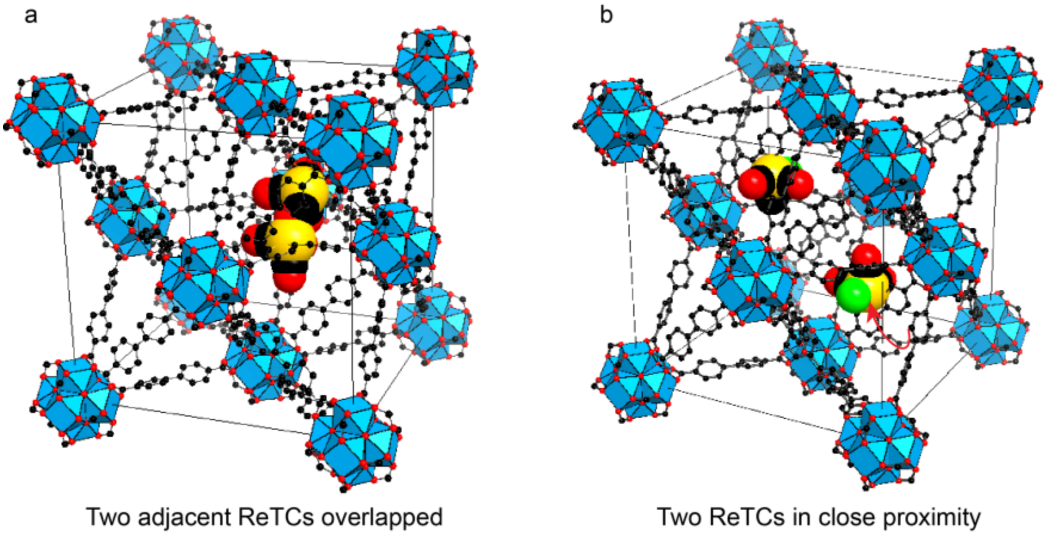

Supporting Figure S17. Structural models showing ReTCs (a) overlapping when n > 4 on adjacent linkers and (b) in close proximity by their free rotation allowing a bimolecular reaction pathway to occur when n < 4, with ReTCs on opposite linkers but in the same octahedral cavity. Other ReTCs beside those presented in (a) are omitted for clarity.

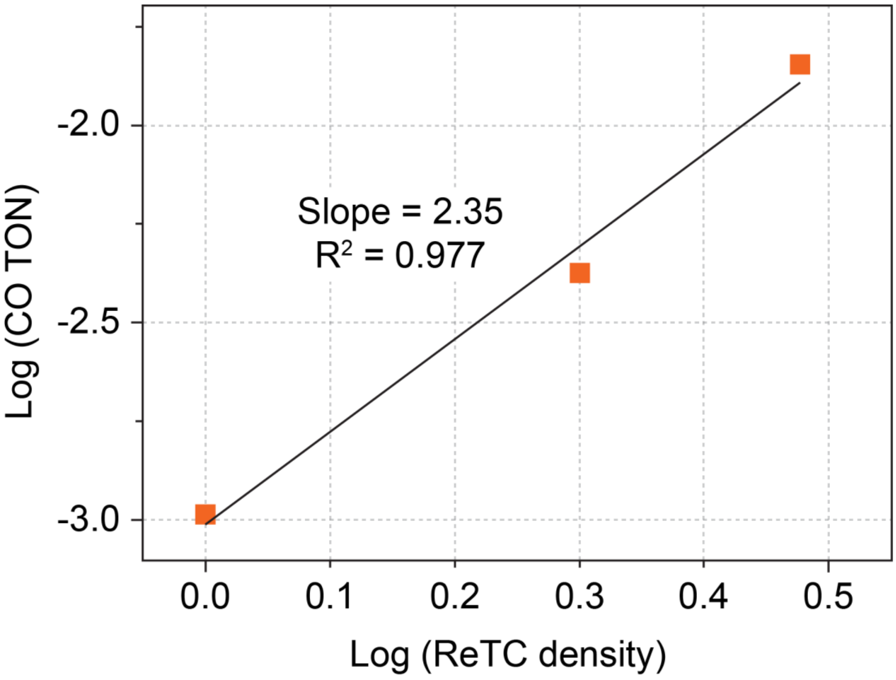

Supporting Figure S18. Reaction order analysis of Re_n-MOFs (from n = 1 to n = 3)

Supporting Section S4. *Characterization of Ag⊂Re₃-MOF*

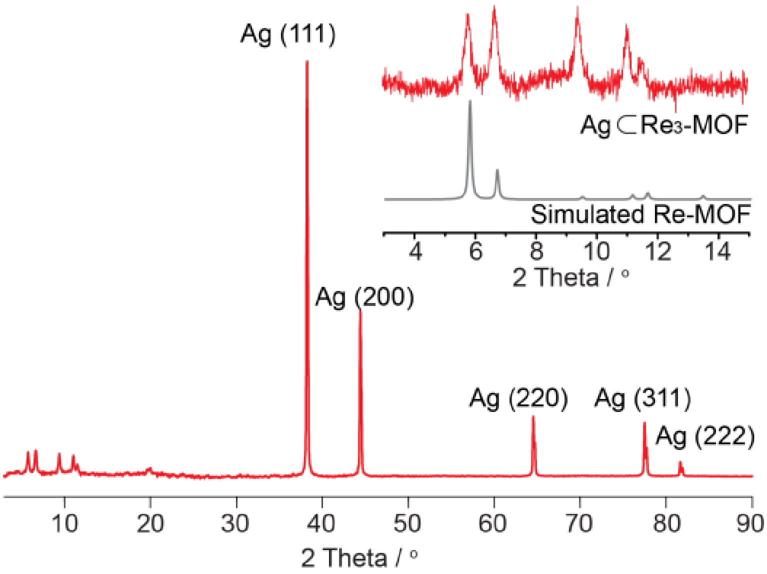

Supporting Figure S19. PXRD of Ag⊂Re$_3$-MOF

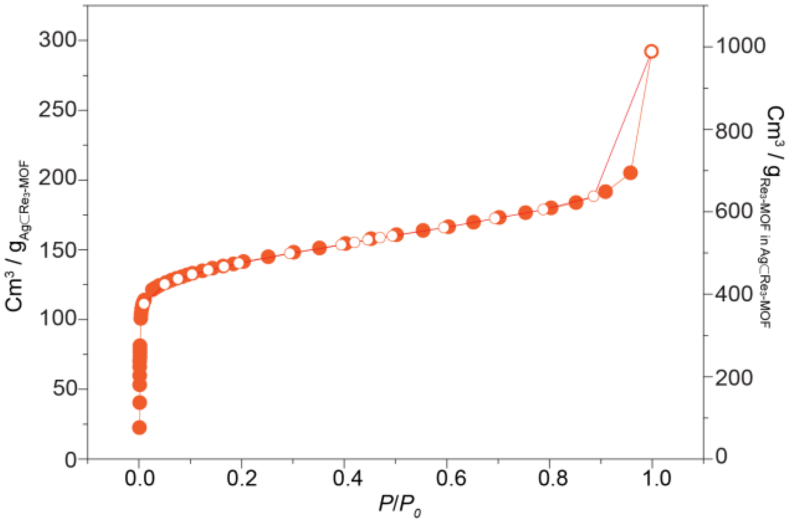

Supporting Figure S20. N_2 sorption isotherm of Ag⊂Re$_3$-MOF at 77 K with adsorption and desorption points represented by closed and open circles, respectively (P/P_0, relative pressure).

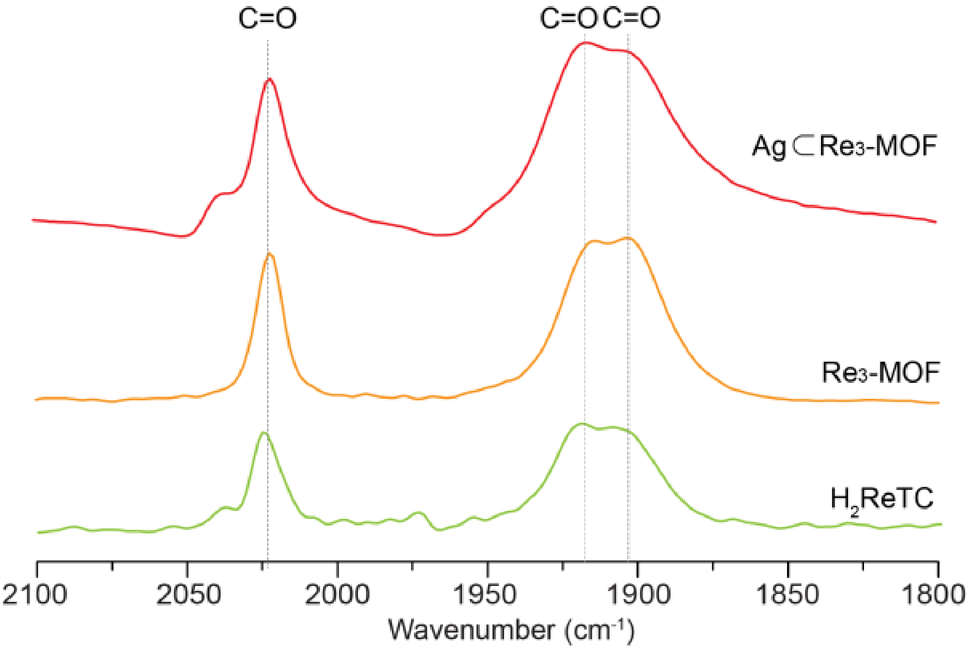

Supporting Figure S21. IR spectra of Ag⊂Re_3-MOF, Re_3-MOF and H_2ReTC

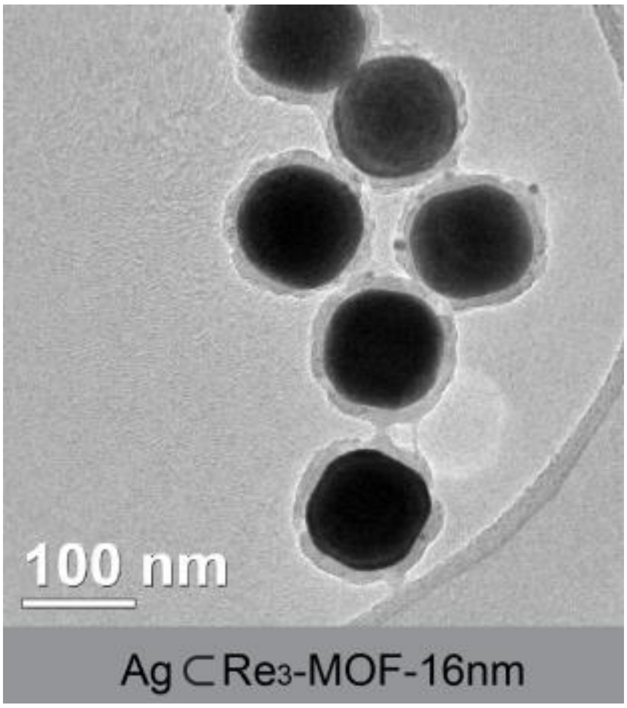

Supporting Figure S22. TEM image of Ag⊂Re_3-MOF with a 16 nm thick Re-MOF layer

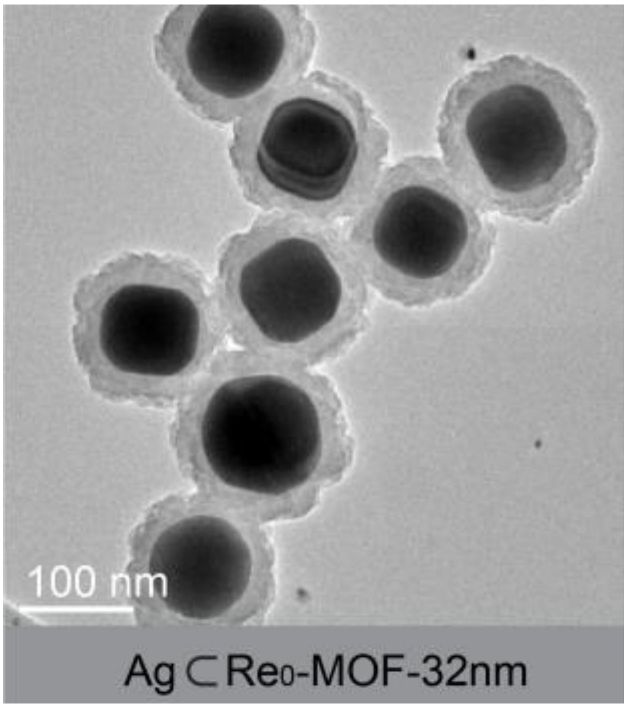

Supporting Figure S23. TEM image of Ag$\subset$Re$_0$-MOF

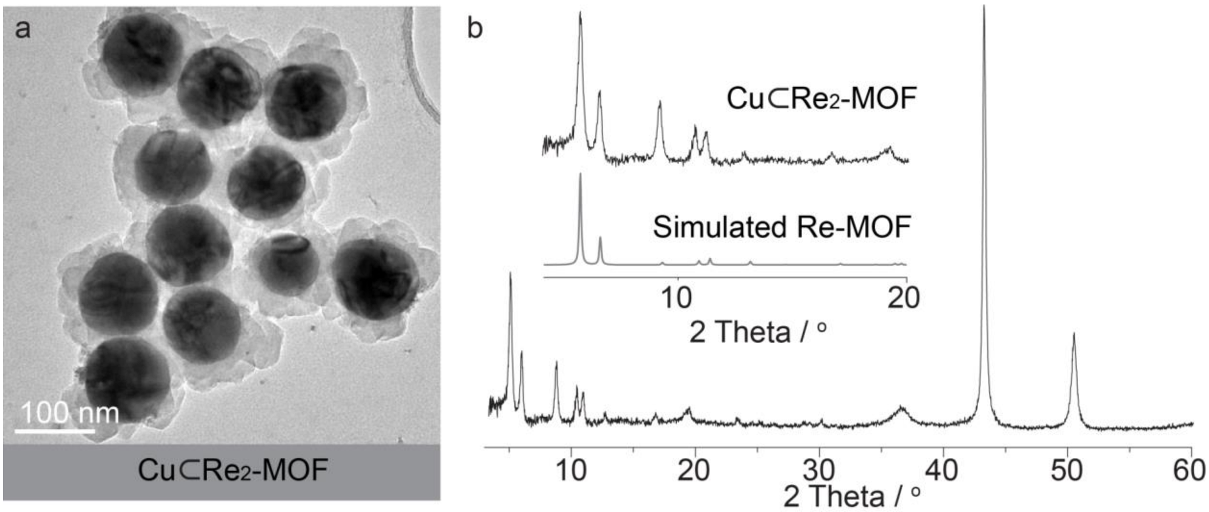

Supporting Figure S24. (a) TEM image and **(b)** PXRD of Cu$\subset$Re$_2$-MOF

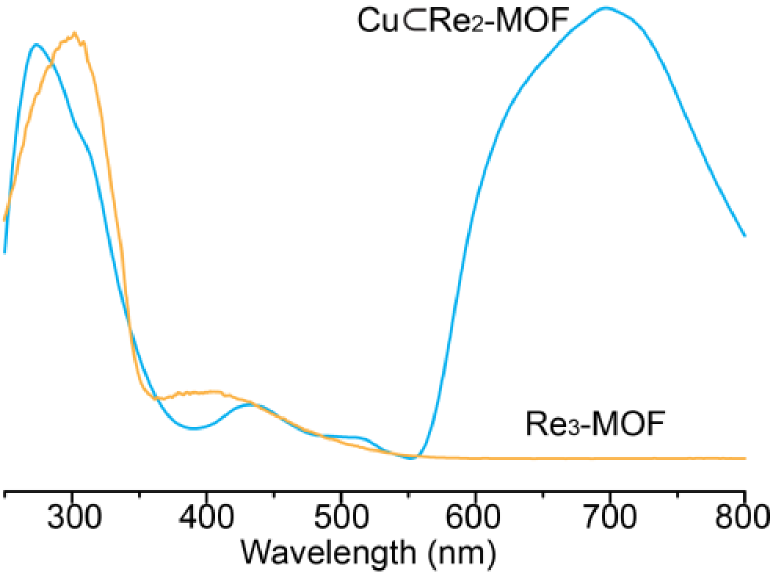

Supporting Figure S25. UV-Vis spectra of Cu⊂Re$_2$-MOF and Re$_3$-MOF. The broad absorption between 600 to 800 nm is from the SPR of Cu nanoparticles.

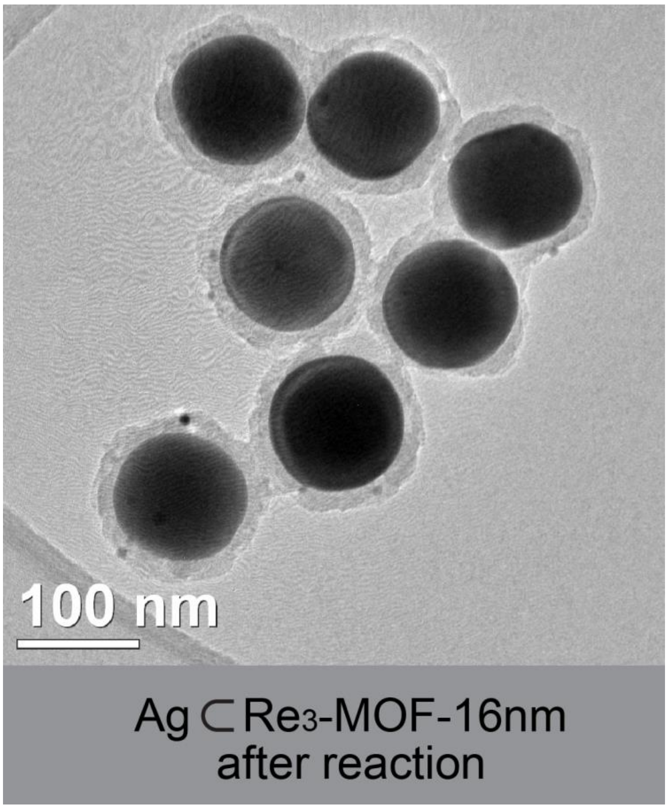

Supporting Figure S26. TEM image of Ag⊂Re$_3$-MOF after the 24 h reaction

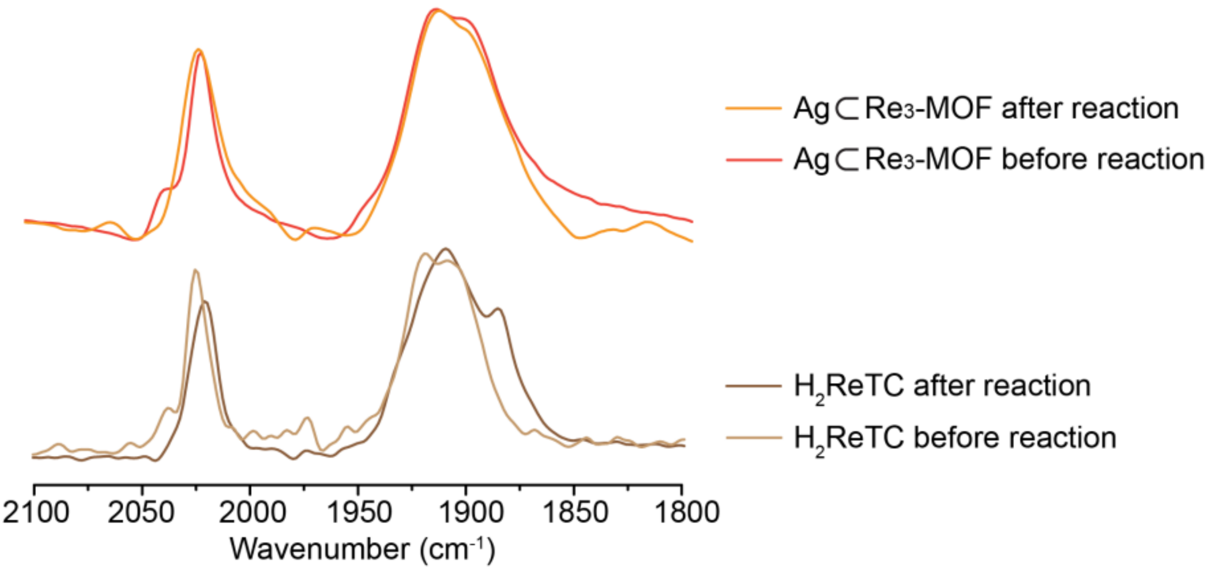

Supporting Figure S27. IR spectra of the Ag⊂Re_3-MOF and H_2ReTC before and after the 24 h reaction